Crystal-field levels in the distorted perovskite $PrGaO_3$

1994 J. Phys.: Condens. Matter 6 4099

(http://iopscience.iop.org/0953-8984/6/22/009)

J. Phys.: Condens. Matter 6 (1994) 4099–4106. Printed in the UK

Crystal-field levels in the distorted perovskite $PrGaO_3$

A Podlesnyak†§, S Rosenkranz†, F Fauth†, W Marti†, H J Scheel‡ and A Furrer†

† Laboratory for Neutron Scattering, Eidgenössische Technische Hochschule Zürich & Paul Scherrer Institute, CH-5232 Villigen PSI, Switzerland

‡ Crystal Growth Group, Institute of Micro- and Optoelectronics, Ecole Polytechnique Fédérale Lausanne, CH-1007 Lausanne, Switzerland

Received 21 October 1993, in final form 3 February 1994

Abstract. Inelastic neutron scattering has been employed to study the crystalline-electric-field interaction of the distorted perovskite $PrGaO_3$. The observed energy spectra show several well defined inelastic peaks of magnetic origin in an energy transfer range up to 86 meV which are attributed to crystalline-electric-field transitions within the ground-state J multiplet $^3H_4$ of the Pr^{3+} ions. The spectra are analysed in terms of single-particle crystal-field theory based on geometrical coordinations associated with the C_s site symmetry of the Pr^{3+} ions. J mixing as well as the imaginary part of the crystal-field Hamiltonian are found to be important to reproduce the experimental data. The resulting crystal-field parameters are close to the values extrapolated from a similar study of $NdGaO_3$. Our approach turns out to constitute a useful extrapolation scheme for other structurally related perovskite-type compounds.

1. Introduction

A detailed knowledge of the crystalline-electric-field (CEF) interaction of the rare-earth ions in the perovskite-type compounds RMO_3 (R = rare earth; M = Ni, Al, Ga) is indispensable for understanding the thermodynamic magnetic properties such as the Schottky anomaly of the specific heat, the magnetization, and the anisotropy of the magnetic susceptibility as well as the various structural and magnetic phase transitions. Since the discovery of high-temperature superconductivity there is increasing interest in the electronic and magnetic properties of oxides having perovskite-type structures. The RMO_3 compounds have been widely studied by various experimental methods such as transport properties [1, 2], electronic Raman effect [3–5], specific heat [6], optical spectroscopy [3, 4], x-ray absorption spectroscopy [7], and neutron scattering [8–11]. In particular, the investigation of the CEF interaction reveals important information about the peculiarities of the electronic structure and plays a key role in determining the magnetic ground state.

Measurements of the CEF splitting in $NdGaO_3$ by inelastic neutron scattering (INS) have been reported recently [9]. They showed that the single-particle CEF theory based on geometrical coordinations associated with the real symmetry of Nd^{3+} adequately explains the majority of magnetic and CEF properties of this compound. The aim of the present paper is to discuss new INS measurements of the CEF splitting in the distorted perovskite $PrGaO_3$. To our knowledge there is no experimental information about other physical properties of $PrGaO_3$ in the current literature.

§ Permanent address: Institute for Metal Physics, Russian Academy of Sciences, Ekaterinburg GSP-170, Russia.

0953-8984/94/224099+08$19.50

2. Experimental details

A single crystal of $PrGaO_3$ was grown by standard Czochralski pulling. Part of the crystal was used for the preparation of the polycrystalline material.

The neutron-scattering measurements were carried out at the reactor Saphir in Würenlingen (Switzerland). For the structural studies the double-axis-multicounter (DMC) diffractometer was used [12]. The INS experiments were performed in the neutron energy-loss configuration with use of the triple-axis spectrometer IN2. The analyser energy was fixed at 15 meV, and a pyrolitic-graphite filter was inserted into the outgoing neutron beam to reduce higher-order contamination. For zero energy transfer the energy resolution was $\Delta E \simeq 1.2$ meV. The $PrGaO_3$ powder sample (15 g) was enclosed in a cylindrical V or Al container (12 mm diameter, 40 mm length) for the neutron-diffraction or spectroscopy experiments, respectively, and mounted in a closed-cycle He refrigerator to achieve temperatures $T \geqslant 12$ K.

3. Results

The $PrGaO_3$ compound crystallizes in the orthorhombic $GdFeO_3$ perovskite-type structure. Our neutron-diffraction study shows that the ideal cubic symmetry of the perovskite is significantly distorted leading to a lower-symmetry structure (space group D_{2h}^{16}—$Pbnm$). There is no indication of any phase transition in the temperature region $10 < T < 300$ K. The Pr^{3+} ions occupy the 4c sites (site symmetry C_s—m). Table 1 lists the structural parameters obtained by the Rietveld refinement. Details of the structure analysis have been reported elsewhere [10].

Table 1. Structural parameters of $PrGaO_3$ at $T = 12$ K: lattice parameters a, b, c and atomic coordinates x, y, z.

a (Å)	5.4526 ± 0.0002		
b (Å)	5.4947 ± 0.0002		
c (Å)	7.7121 ± 0.0003		
	x	y	z
Pr	-0.0065 ± 0.0009	-0.0386 ± 0.0004	0.2500
Ga	0.5	0.0	0.0
O1	0.0786 ± 0.0005	0.5164 ± 0.0004	0.25
O2	-0.2123 ± 0.0003	0.2109 ± 0.0003	0.0419 ± 0.0002

The INS spectra taken at $T = 12$ K exhibit five well resolved inelastic lines at 5.1, 16.0, 21.5, 67 and 86 meV, whose line widths correspond to the instrumental resolution; in addition, there is evidence of a broad inelastic feature at 38 meV. Representative energy spectra are shown in figures 1 and 2. We can interpret the six inelastic lines (A–F) in terms of CEF transitions out of the ground state, since the phonon density of states of the non-magnetic reference compound $LaGaO_3$ measured at $T = 150$ K was found to exhibit little inelastic intensity in the considered energy-transfer range (see figures 1 and 2). Moreover, CEF transitions can be identified by the way in which their intensities vary with temperature and modulus of the scattering vector Q. As the temperature rises, the phonon intensities increase, whereas the intensities of CEF ground-state transitions decrease due to the depopulation of the ground state. In addition, we expect to observe CEF transitions out

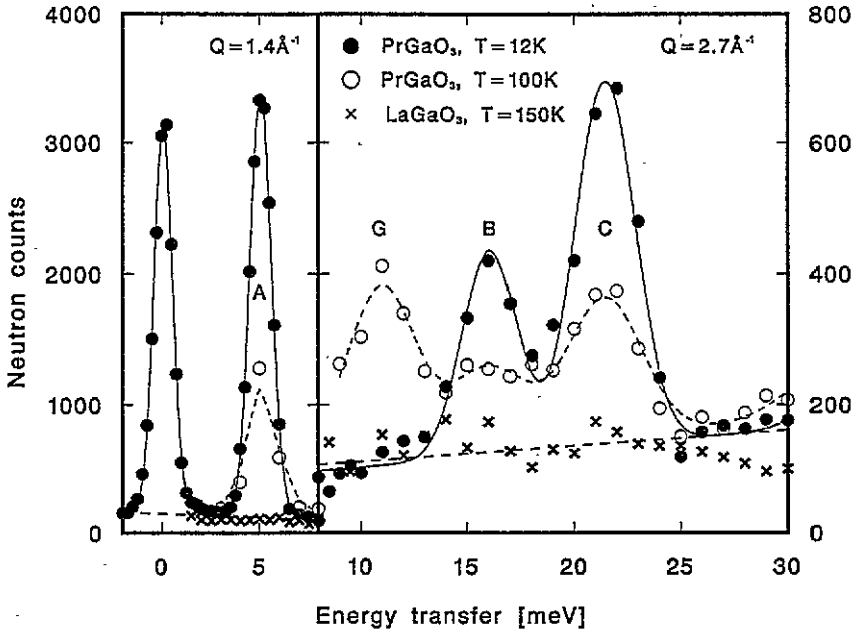

Figure 1. Energy spectra of neutrons scattered from $PrGaO_3$ and $LaGaO_3$. The lines are the result of a least-squares-fitting procedure in which the CEF transitions are described by single Gaussians and the background has been assumed to be linear.

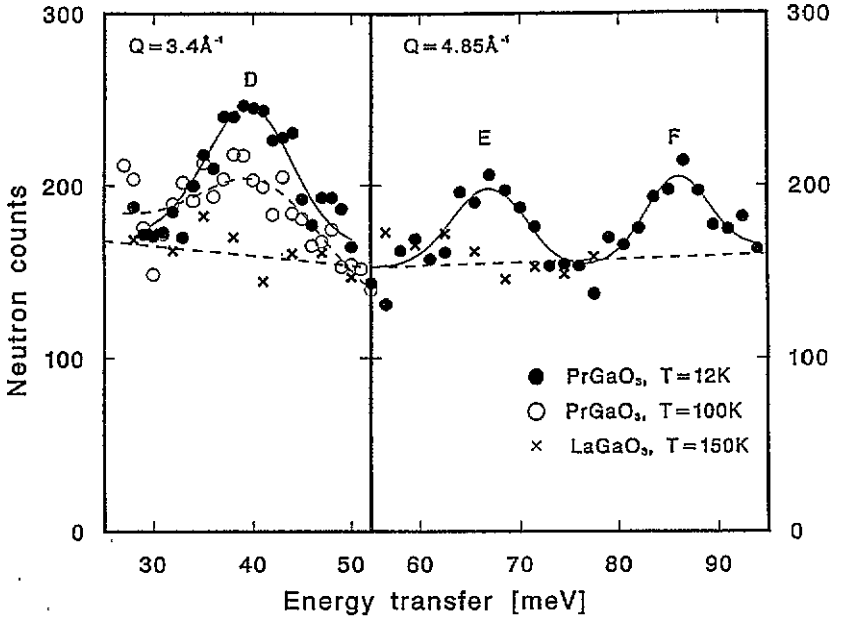

Figure 2. Energy spectra of neutrons scattered from $PrGaO_3$ and $LaGaO_3$. The lines are as in figure 1.

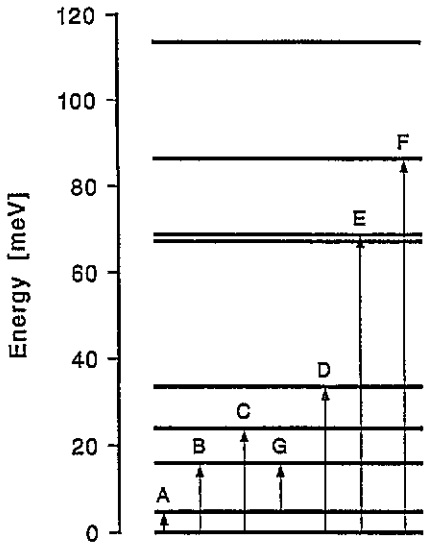

Figure 3. Calculated energy-level scheme of Pr^{3+} in $PrGaO_3$. The arrows denote the observed CEF transitions.

of excited states at elevated temperatures (peak G in figure 1). On the other hand, the intensities of CEF transitions decrease with increasing value of Q due to the magnetic form factor, whereas phonon intensities usually increase.

The ninefold degeneracy of the ground-state J multiplet $^3H_4$ of the Pr^{3+} ions in $PrGaO_3$ is completely lifted by the CEF. Thus, in the present INS experiments we have been able to observe the majority of the CEF transitions out of the ground state and thereby to assign the energies of six among the eight excited CEF levels (see figure 3).

4. Crystal-field analysis

The CEF analysis was carried out in the framework of single-particle crystal-field theory [13]. The corresponding Hamiltonian is given by

$$H_{\mathrm{CEF}} = \sum_{k,q,i} A_q^{(k)} C_q^{(k)}(i) \tag{1}$$

where $A_q^{(k)}$ is a CEF parameter and $C_q^{(k)}(i)$ is a spherical tensor operator of rank k depending on the coordinates of the ith electron. The summation involving i is over all f electrons of the R ion. The indices k and q for which the parameters $A_q^{(k)}$ are non-zero depend on the site symmetry. Usually the CEF potential is treated as a perturbation of the ground-state J multiplet alone. However, for the $PrGaO_3$ compound examined here, the overall CEF splitting is about 120 meV and therefore comparable to the energy separation from the next J multiplet (approximately 250 meV), thus we have included intermultiplet interactions within the ^3H term in our calculations. A crystal-field formalism considering the ground-state J multiplet alone has been introduced by Stevens [14]:

$$H_{\mathrm{CEF}} = \sum_{n,m,\alpha} B_n^{m(\alpha)} O_n^m(i) \qquad (\alpha = \mathrm{c}, \mathrm{s}) \tag{2}$$

where $B_n^{m(\alpha)}$ is a CEF parameter and $O_n^m(i)$ an operator equivalent. $B_n^{m(\mathrm{c})}$ and $B_n^{m(\mathrm{s})}$ correspond to the real and imaginary parts of the CEF parameters, respectively. The CEF

Table 2. Geometrical coordination factors for the Pr^{3+} site in $PrGaO_3$ calculated from the neutron-diffraction data as explained in the text.

n	m	$\gamma_n^{m(c)}$ (Å$^{-(n+1)}$)	$\gamma_n^{m(s)}$ (Å$^{-(n+1)}$)
4	0	0.12×10^{-2}	—
4	2	0.24×10^{-2}	-0.14×10^{-1}
4	4	-0.44×10^{-2}	0.15×10^{-1}
6	0	0.34×10^{-3}	—
6	2	-0.59×10^{-3}	-0.12×10^{-2}
6	4	0.83×10^{-2}	0.04×10^{-3}
6	6	-0.12×10^{-2}	0.27×10^{-3}

parameters $A_q^{(k)}$ of (1) can easily be transformed into the CEF parameters $B_n^{m(\alpha)}$ of (2) by using normalizing coefficients [15]. Throughout this paper we will use the CEF parameters $B_n^{m(\alpha)}$ of the Stevens operator formalism.

Perovskites are known as model systems in solid-state physics because of their relatively simple structure. However, the interpretation of INS data for these materials is by no means straightforward. The rather low symmetry at the rare-earth site gives rise to a large number of independent CEF parameters $B_n^{m(\alpha)}$; in particular, the CEF potential of C_s symmetry at the Pr^{3+} site in $PrGaO_3$ is characterized by fifteen independent CEF parameters. Although both the energies and the intensities can be used in fitting a crystal-field model, we cannot initially determine so many CEF parameters and we have to introduce some approximations. To our knowledge, the CEF approximations adopted so far for different RMO_3 compounds were always based on the C_v (or higher) symmetry rather than on the real symmetry (see [3–5] and [8]). Indeed, the number of parameters can be reduced in this way. However, these approximations cannot provide a full understanding of the energy level structure of the R^{3+} ions in $RGaO_3$, because the low-symmetry environment yields significant contributions to the imaginary part of the CEF Hamiltonian. Therefore we have used another approach. As repeatedly shown in the past for several perovskite-type compounds [16–19], the CEF parameters $B_n^{m(\alpha)}$ for $n \geqslant 4$ may reasonably be determined by taking into account the geometry of the nearest-neighbouring coordination polyhedron:

$$B_n^{m(\alpha)} = (\gamma_n^{m(\alpha)}/\gamma_n^0)B_n^0 \qquad (\alpha = \mathrm{c}, \mathrm{s}). \tag{3}$$

The coordination factors $\gamma_n^{m(\alpha)}(\alpha = \mathrm{c}, \mathrm{s})$ are defined by Hutchings [20]. Neutron-diffraction measurements [9, 10] showed that for $RGaO_3$ there is a considerable spread of the radial extension of the coordination polyhedra around the R^{3+} ion. From the structural information for $PrGaO_3$ listed in table 1 we derive the following ranges of the three nearest-neighbouring shells associated with the O^{2-}, Ga^{3+}, and Pr^{3+} ligand ions:

$$2.357 < R(Pr^{3+}\text{–}O^{2-}) < 3.300 \text{ Å}$$

$$3.185 < R(Pr^{3+}\text{–}Ga^{3+}) < 3.532 \text{ Å}$$

$$3.819 < R(Pr^{3+}\text{–}Pr^{3+}) < 3.923 \text{ Å}.$$

More distant coordination shells have interatomic distances larger than 4.45 Å. We have therefore included the three nearest-neighbouring coordination polyhedra in the calculation of the geometry factors $\gamma_n^{m(\alpha)}$ by properly weighting with the nominal charges of the ligand ions. The resulting coordination factors are listed in table 2. The second-order parameters $B_2^{m(\alpha)}$ are not well estimated by this way, because they are governed by long-range electrostatic contributions. We have therefore allowed the three CEF parameters B_2^0, $B_2^{2(c)}$ and $B_2^{2(s)}$ to vary independently.

Table 3. Observed and calculated energy levels and normalized transition probabilities of the CEF states in $PrGaO_3$. J_p denotes the component of the total angular momentum operator perpendicular to the scattering vector Q.

$\Gamma^{(j)}$	E_{obs} (meV)	E_{calc} (meV)	$\lvert\langle\Gamma^{(j)}\rvert J_p \rvert\Gamma^{(1)}\rangle\rvert^2_{obs}$	$\lvert\langle\Gamma^{(j)}\rvert J_p \rvert\Gamma^{(1)}\rangle\rvert^2_{calc}$
$\Gamma^{(1)}$	—	0	—	—
$\Gamma^{(2)}$	5.1 ± 0.1	5.6	1.0	1.0
$\Gamma^{(3)}$	16.0 ± 0.2	16.0	0.25 ± 0.1	0.19
$\Gamma^{(4)}$	21.5 ± 0.2	23.4	0.5 ± 0.1	0.60
$\Gamma^{(5)}$	38.0 ± 2.0	32.9	0.2 ± 0.2	0.31
$\Gamma^{(6)}$	—	67.4	0	0.02
$\Gamma^{(7)}$	67.0 ± 2.0	69.3	0.4 ± 0.2	0.30
$\Gamma^{(8)}$	86.0 ± 2.0	85.8	0.3 ± 0.2	0.17
$\Gamma^{(9)}$	—	113.1	0	0.0

The most difficult problem of any non-linear least-squares-fitting procedure is a reasonable choice for the start values of the fitting parameters. We have started from the CEF parameters B_2^0, B_4^0 and B_6^0 based on our detailed measurements of $NdGaO_3$ [9]. Then we have extrapolated these values to the parameters expected for $PrGaO_3$ by the usual relation:

$$B_n^0 = a_n^0 \langle r^n \rangle \chi_n \gamma_n^0 \tag{4}$$

where $\langle r^n \rangle$ is the nth moment of the radial distribution of the 4f electrons [21], χ_n is a reduced matrix element [15], and a_n^0 is a reduced CEF parameter reflecting the charge distribution independent of the particular rare-earth ion. From (4) we derive

$$B^0_{n(Pr^{3+})} = B^0_{n(Nd^{3+})} \langle r^n \rangle_{(Pr^{3+})} \chi_{n(Pr^{3+})} \gamma^0_{n(Pr^{3+})} / \langle r^n \rangle_{(Nd^{3+})} \chi_{n(Nd^{3+})} \gamma^0_{n(Nd^{3+})}. \tag{5}$$

Thus, using these constraints we are left with five independent CEF parameters which were then varied in the least-squares-fitting procedure. The best convergence was achieved for the following CEF parameters:

$$B_2^0 = -0.90 \pm 0.05 \text{ meV}$$

$$B_2^{2(c)} = -0.17 \pm 0.05 \text{ meV}$$

$$B_2^{2(s)} = 0.23 \pm 0.05 \text{ meV}$$

$$B_4^0 = (0.46 \pm 0.02) \times 10^{-2} \text{ meV}$$

$$B_6^0 = (-0.36 \pm 0.01) \times 10^{-3} \text{ meV}.$$

The off-diagonal fourth- and sixth-order CEF parameters were fixed according to (3). Figure 3 and table 3 show the calculated CEF level scheme, which is in good agreement with the observations. Table 3 also lists the normalized observed and calculated transition probabilities, which are found to agree as well. There is only some disagreement with respect to the energy of the $\Gamma^{(5)}$ level. The corresponding ground-state transition turned out to be anomalously broad (see figure 2), similar to $NdBa_2Cu_3O_7$ [22] where the broadening of the CEF line at around 36 meV has been shown to result from an interaction with the phonons. We may encounter the same situation here.

5. Discussion and concluding remarks

We would like to point out two particular points. Firstly, we emphasize the role of the imaginary part of the CEF Hamiltonian in the low-symmetry $RGaO_3$ compounds. Our attempts to determine the CEF level structure in these systems from higher-symmetry considerations clearly failed. Secondly, the final parameters B_4^0 and B_6^0 determined for $PrGaO_3$ agreed within experimental uncertainty with those extrapolated from $NdGaO_3$ according to (4). In other words, the actual charge distributions (reflected in the reduced CEF parameters a_n^0) are found to be very similar for both $NdGaO_3$ and $PrGaO_3$. Table 4 lists also reduced CEF parameters for other perovskite-type RMO_3 compounds. The resulting values of a_n^0 turn out to be reasonably consistent, although the tilt angle of the O octahedra is much larger for the gallates than, e.g., for the aluminates.

Table 4. Reduced CEF parameters a_4^0 and a_6^0 for different RMO_3 compounds.

	$PrGaO_3$	$NdGaO_3$	$PrAlO_3$	$NdAlO_3$
Reference	this work	[9]	[5]	[3]
a_4^0 (10^4 meV Å)	-2.4 ± 0.2	-2.4 ± 0.3	-1.7 ± 0.2	-1.9
a_6^0 (10^4 meV Å)	-4.9 ± 0.2	-4.6 ± 0.3	-3.3 ± 0.3	-4.2

In conclusion, we have presented the results of INS measurements of the CEF transitions associated with the Pr^{3+} ions in $PrGaO_3$. We have been able to determine a set of CEF parameters based on geometrical coordinations describing the real symmetry at the Pr^{3+} site. The reduced CEF parameters resulting from the present work may conveniently be used to extrapolate the CEF interaction to other RMO_3 compounds; however, for a detailed understanding of the CEF level structure it is essential to take account of the real symmetry around the R^{3+} ions.

Acknowledgment

One of the authors (AP) is grateful to the Swiss National Science Foundation for financial support of a post-doctoral position.

References

[1] Granados X, Fontcuberta J, Obradors X and Torrance J B 1992 *Phys. Rev.* B **46** 15 683
[2] Xu X Q, Peng J L, Li Z Y, Ju H L and Greene R L 1993 *Phys. Rev.* B **48** 1112
[3] Finkman E, Cohen E and Van Uitert L G 1973 *Phys. Rev.* B **7** 2899
[4] Harley R T, Hayes W, Perry A M and Smith S R P 1973 *J. Phys. C: Solid State Phys.* **6** 2382
[5] Lyons K B, Birgeneau R J, Blount E I and Van Uitert L G 1975 *Phys. Rev.* B **11** 891
[6] Bartolomé F, Kuz'min M D, Merino R J and Bartolomé J to be published
[7] Medarde M, Fontaine A, García-Muñoz J L, Rodríges-Carvajal J, de Santis M, Sacchi M, Rossi G and Lacorre P 1992 *Phys. Rev.* B **46** 14 975
[8] Birgeneau R J, Kjems J K, Shirane G and Van Uitert L G 1974 *Phys. Rev.* B **10** 2512
[9] Podlesnyak A, Rosenkranz S, Fauth F, Marti W, Furrer A, Mirmelstein A and Scheel H J 1993 *J. Phys.: Condens. Matter* **5** 8973
[10] Marti W, Fischer P, Altorfer F, Scheel H J and Tadin M 1994 *J. Phys.: Condens. Matter* **6** 127
[11] Marti W, Medarde M, Rosenkranz S, Roessli B, Fischer P, Furrer A and Scheel H J *Phys. Rev.* B submitted

[12] Schefer J, Fischer P, Heer H, Isacson A, Koch M and Thut R 1990 *Nucl. Instrum. Methods* A **288** 477
[13] Wybourne B G 1965 *Spectroscopic Properties of Rare Earths* (New York: Interscience)
[14] Stevens K W H 1952 *Proc. Phys. Soc.* A **65** 209
[15] Dieke G H 1965 *Spectra and Energy Levels of Rare Earth Ions in Crystals* (New York: Interscience)
[16] Furrer A, Brüesch P and Unternährer 1988 *Phys. Rev.* B **38** 4616
[17] Podlesnyak A, Kozhevnikov V, Mirmelstein A, Allenspach P, Mesot J, Staub U, Furrer A, Osborn R, Bennington S M and Taylor A D 1991 *Physica* C **175** 587
[19] Mesot J, Allenspach P, Staub U, Furrer A and Mutka H 1993 *Phys. Rev. Lett.* **70** 865
[20] Hutchings M T 1964 *Solid State Physics* vol 16, ed F Seitz and D Turnbull (New York: Academic) p 227
[21] Freeman A J and Watson R E 1962 *Phys. Rev.* **127** 2058
[22] Heyen E T, Wegerer R, Schönherr E and Cardona M 1991 *Phys. Rev.* B **44** 10 195